Rapid Communications

Signatures of quantum mechanical Zeeman effect in classical transport due to topological properties of two-dimensional spin-$\frac{3}{2}$ holes

E. Marcellina,[1,*] Pankaj Bhalla,[2] A. R. Hamilton,[1] and Dimitrie Culcer[1]

[1]*School of Physics and Australian Research Council Centre of Excellence in Future Low-Energy Electronics Technologies, The University of New South Wales, Sydney 2052, Australia*

[2]*Beijing Computational Science Research Center, Beijing 100193, China*

(Received 23 July 2019; revised manuscript received 19 February 2020; accepted 20 February 2020; published 9 March 2020)

The Zeeman interaction is a quantum mechanical effect that underpins spin-based quantum devices such as spin qubits. Typically, identification of the Zeeman interaction needs a large *out-of-plane* magnetic field coupled with ultralow temperatures, which limits the practicality of spin-based devices. However, in two-dimensional (2D) semiconductor holes, the strong spin-orbit interaction causes the Zeeman interaction to couple the spin, the magnetic field, and the momentum, and has terms with different winding numbers. In this work, we demonstrate a physical mechanism by which the Zeeman terms can be detected in classical transport. The effect we predict is very strong, and tunable by means of both the density and the in-plane magnetic field. It is a direct signature of the topological properties of the 2D hole system, and a manifestation in classical transport of an effect stemming from relativistic quantum mechanics. We discuss experimental observation and implications for quantum technologies.

DOI: 10.1103/PhysRevB.101.121302

Recent years have witnessed the rapid development of materials and structures in which relativistic quantum mechanical effects, such as the spin-orbit interaction, play a dominant role in future spin-based device concepts [1–4]. A natural place where such effects are important is state-of-the-art semiconductor hole devices [5–24]. The impressive progress in this field over this decade is motivated by the intense interest in hole systems as building blocks in quantum computing architectures and as the next generation of nanoscale topological devices [25–36]. The strong spin-orbit coupling in holes [37–44] together with weak hyperfine interactions enable low-power electrical spin manipulation [45,46] and long coherence times [11,47–49]. Furthermore, strongly spin-orbit coupled systems can exhibit proximity-induced superconductivity [50], which can open a pathway towards topological quantum computation via Majorana bound states with non-Abelian statistics [51–56]. However, a challenge that can limit the practicality of spin-based devices is that the detection of spin states often requires a large magnetic field and/or ultralow temperatures [6–19,35,36,44,50,57]. In light of this it is natural to investigate the signatures of spin in classical transport.

In this work we examine the signatures of the Zeeman interaction, which is fundamental to spin qubit dynamics, spin-based quantum information processing, and Majorana states in semiconductor-superconductor hybrids, in classical transport. We find that, in strongly spin-orbit coupled systems, the Zeeman interaction has a significant and measurable effect on the classical magnetoresistance. Our model system is a two-dimensional hole gas (2DHG) in a symmetric quantum well, subject to a weak out-of-plane magnetic field B_z (of order milliteslas) and a sizable in-plane magnetic field (B_x, B_y) (of the order of a few teslas), where the Rashba spin-orbit interaction [58] is absent. As Fig. 2 shows, the Zeeman interaction with an in-plane magnetic field gives rise to a sizable anisotropy in both the longitudinal conductivity and the Hall coefficient, implying, in particular, that the Hall coefficient in this case is not simply a measure of the carrier density and is strongly influenced by the Zeeman interaction. Fundamentally this effect occurs because, unlike spin-$\frac{1}{2}$ electrons, holes are described by an effective spin-$\frac{3}{2}$. This means that there are four possible projections onto the spin quantization axis (i.e., the axis perpendicular to the interface, denoted here by z). The projections $m_J = \pm 3/2$ ($m_J = \pm 1/2$) have a heavier (lighter) effective mass, thus these states are termed as heavy (light) holes. Since, in two dimensions, the heavy holes projection is parallel to the z axis, they exhibit a peculiar Zeeman interaction with an in-plane magnetic field $B_\parallel$, which couples the spin simultaneously to the external magnetic field and to the momentum k. It has long been known that a term $\propto B_\parallel k^2$ exists quadratic in the wave vector $\boldsymbol{k}$ [37], while recently a new term $\propto B_\parallel k^4$ was predicted [59] and experimentally identified [57]. These two terms have different winding directions and make large contributions to the velocity operator and hence to the current. The higher-order coupling between $B_\parallel$ and k also manifests in an extremely density-dependent in-plane g factor, whereby we have demonstrated that the g factor became enhanced by 300% as the density was tripled [44].

*Present address: School of Physical and Mathematical Sciences, Nanyang Technological University, 21 Nanyang Link, Singapore 637371; emarcellina@ntu.edu.sg

Assuming that only the lowest (i.e., zero-node) heavy hole subbands are occupied, which is often the case experimentally, the band Hamiltonian with in-plane Zeeman terms is

$$H_{0\boldsymbol{k}} = \frac{\hbar^2 k^2}{2m^*} + \Delta_1 B_+ k_+^2 \sigma_- + \Delta_2 B_- k_+^4 \sigma_- + \text{H.c.}, \quad (1)$$

where the first term is the orbital term with m^* an effective hole mass and the remaining part, known as the Zeeman Hamiltonian, is equivalent to $\frac{1}{2}\boldsymbol{\sigma}\cdot\boldsymbol{\Omega_k}$ having

$$\hat{\boldsymbol{\Omega}}_{\boldsymbol{k}} = \frac{\Delta_1 k^2 B_\parallel (c_{2\theta+\phi} + \Delta k^2 c_{4\theta-\phi}, s_{2\theta+\phi} + \Delta k^2 s_{4\theta-\phi}, 0)}{\sqrt{G(k)}}, \quad (2)$$

$k_\pm \equiv k_x \pm i k_y$, $k \equiv \sqrt{k_x^2 + k_y^2}$, and H.c. denotes the Hermitian conjugate for the Zeeman terms. The prefactors Δ_1 and Δ_2 were calculated for specific structures in Ref. [59] and can be generically determined from $\boldsymbol{k}\cdot\boldsymbol{p}$ theory, the details of which we defer to a future publication. We also use $\Delta \equiv \Delta_2/\Delta_1$, while $B_\pm \equiv B_x \pm i B_y$, with $B_{x(y)}$ the $x(y)$ component of the magnetic field, $\sigma_\pm \equiv \sigma_x \pm i\sigma_y$, with σ_i the Pauli spin matrices, $G(k) \equiv (\Delta_1^2 k^4 + \Delta_2^2 k^8 + 2\Delta_1\Delta_2 k^6 c_{2(\theta-\phi)})B_\parallel^2$, $\theta = \tan^{-1}(k_y/k_x)$, $\phi = \tan^{-1}(B_y/B_x)$, $c(s)$ refers to the cosine(sine) trigonometric operators, and H.c. stands for Hermitian conjugate. We neglect the Dresselhaus spin-orbit interaction [60] and cubic-symmetry Luttinger terms, since these do not change the interaction with the magnetic field. We consider cases where $B_\parallel$ is sufficiently small so that the lowest order Schrieffer-Wolff approximation for the Zeeman interaction [Eq. (1)] remains valid. At a typical density of $p = 1.6 \times 10^{11}$ cm^{-2}, Eq. (1) applies for $B_\parallel \leqslant 3.9$ T and $B_\parallel \leqslant 2.2$ T for GaAs and InAs, respectively. We ignore Landau levels since, for the range of $B_\parallel$ considered in the work, the magnetic length is at least one order of magnitude larger than the spatial overlap of the wave function, i.e., $\sqrt{\hbar/(eB_\parallel)} \gg \langle z \rangle$. We do not include higher-order Zeeman interactions $\propto B_\parallel^3$ [37] since they are approximately three orders of magnitude smaller than the B-linear term, meaning that the $B_\parallel^3$ term only becomes important when $B_\parallel \sim 30$ T.

The peculiar form of the Zeeman interaction in Eq. (1) implies that the in-plane magnetic field in real space becomes an *effective* magnetic field $\boldsymbol{\Omega_k}$ in momentum space. We have plotted this effective field in Figs. 1(a)–1(c). As expected, the texture of the effective field and the energy dispersion are both strongly density dependent. The Δ_1 term has a winding number $w_1 = 2$ and is dominant at lower densities, whereas the Δ_2 term has a winding number $w_2 = 4$ and is dominant at higher densities. Figures 1(d)–1(f) show the Zeeman splitting of the heavy hole subbands, calculated using the dispersion relation $E(k) = \frac{\hbar^2 k^2}{2m^*} \pm \sqrt{G(k)}$ for a typical experimental density of $p = 1.6 \times 10^{11}$ cm^{-2} and $B_\parallel = B_x = 1$ T. If either Δ_1 or Δ_2 is zero [Figs. 1(d) and 1(e)] the energy dispersion is isotropic, while if the two are comparable in magnitude the dispersion is anisotropic [Fig. 1(f)]. The anisotropy in the Fermi contours occurs because of the existence of two terms with different winding numbers. Finally we note that there exists a density and ϕ at which the term $\Delta_1 k^2$ exactly equals $\Delta_2 k^4$. At this point, the term $G(k)$ is zero at $\phi = \pi/2$ and $3\pi/2$, causing the perturbation expansion to fail. This case, which occurs at low densities, is not included in our calculation since it involves a laborious extension of the theory. From the physical standpoint, at the point where $G(k)$ becomes zero the two heavy hole subbands become degenerate, which contradicts our starting assumption that the two subbands are split by the Zeeman interaction and that they have different subband occupations as well as occupation probabilities.

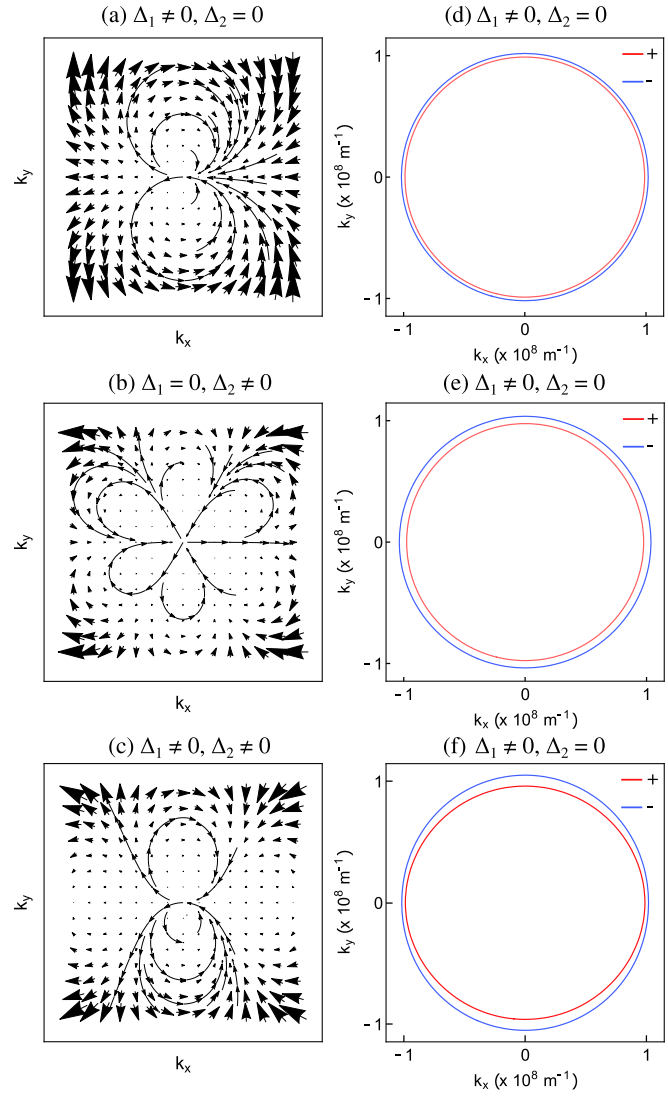

FIG. 1. Schematics for the vector field (Ω_x, Ω_y) with (a) $\Delta_2 = 0$, (b) $\Delta_1 = 0$, and (c) $\Delta_1 k^2 \approx \Delta_2 k^4$ with $B_\parallel = B_x$. The values for Δ_1 and Δ_2 are $\Delta_1 = 1 \times 10^{-17}$ meV m^2 T^{-1} and $\Delta_2 = -2 \times 10^{-33}$ meV m^4 T^{-1}, respectively. The Zeeman splitting for $p = 1.6 \times 10^{11}$ cm^{-2} and $B_\parallel = 1$ T was found to be (d) ~3%, (e) ~6%, and (f) ~6% of the Fermi energy. Here, $+$ $(-)$ refers to $m_J = +3/2$ $(-3/2)$ heavy holes subband. The values for Δ_1 and Δ_2 are taken from Ref. [59].

The momentum-dependent Zeeman terms produce sizable modifications of the longitudinal and Hall conductivities as $B_\parallel$ is increased, as well as a large anisotropy in both as the magnetic field is rotated in the plane of the sample. The strong anisotropy relative to the orientation of magnetic field is shown for GaAs and InAs in Fig. 2 which is the central result of this work. This quantum mechanical effect present for weak momentum scattering, is temperature-independent

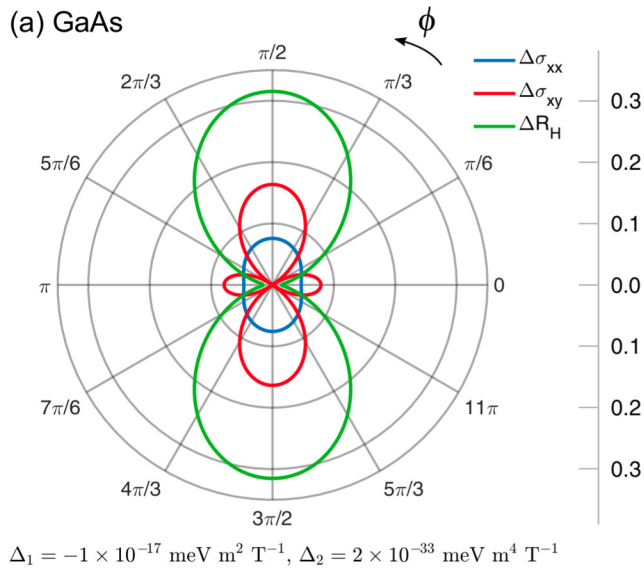

$\Delta_1 = -1 \times 10^{-17}$ meV m^2 T^{-1}, $\Delta_2 = 2 \times 10^{-33}$ meV m^4 T^{-1}

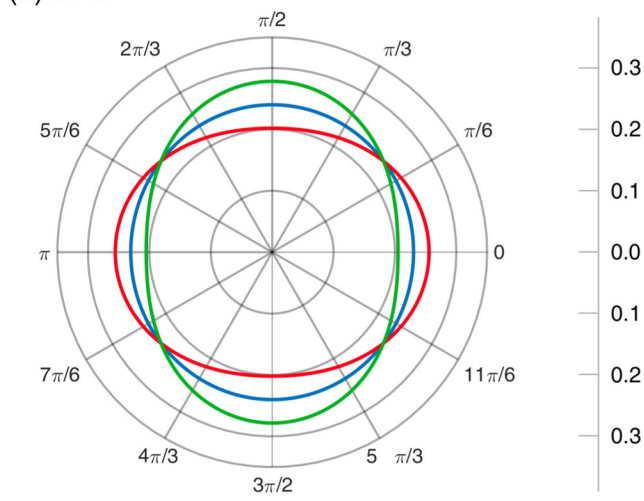

$\Delta_1 = -0.55 \times 10^{-17}$ meV m^2 T^{-1}, $\Delta_2 = 12.58 \times 10^{-33}$ meV m^4 T^{-1}

FIG. 2. The correction for the longitudinal conductivity $\Delta\sigma_{xx}$, transverse conductivity $\Delta\sigma_{xy}$, and Hall coefficient ΔR_H for (a) GaAs and (b) InAs. We define $\Delta R \equiv |R - R_0|/R_0$ where R_0 is the magnetoresistance or Hall resistance at zero magnetic field. Here $k_F = 1 \times 10^8$ m^{-1} and $B_\parallel = 1$ T.

and has a strong density dependence. The angular dependence of the Hall coefficient R_H can be used to identify the presence of the two Zeeman terms. Surprisingly, the Hall coefficient, a classical probe characterizing the interaction with an out-of-plane magnetic field, can be used to characterize the relativistic interaction with an *in-plane* magnetic field. This naturally also in the presence of an in-plane magnetic field, R_H due to an out-of-plane magnetic field is not simply dependent on the carrier density.

The physical reasons behind this effect are as follows. The in-plane magnetic field gives rise to a nontrivial spin texture and to a spin splitting, which renormalizes the Fermi velocity of the spin-split subbands, as well as inter- and intraband scattering times. The net effect of these processes is a sizable renormalization of the Lorentz force acting on the holes. This

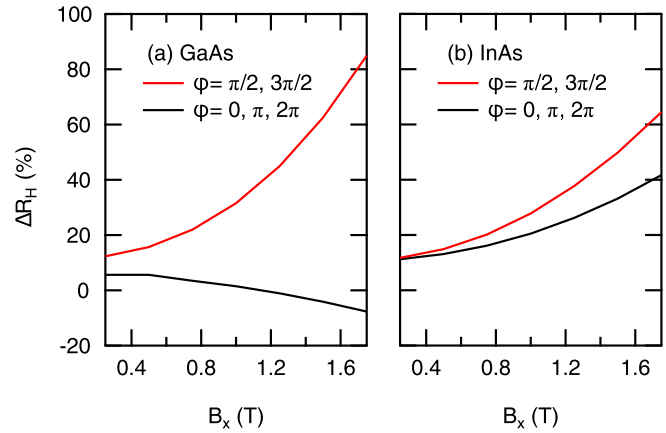

FIG. 3. The extrema of ΔR_H for (a) GaAs and (b) InAs as a function of the in-plane magnetic field B_x; $k_F = 10^8$ m^{-1}.

is surprising for three fundamental reasons. Firstly, $B_\parallel$ does not contribute directly to the Lorentz force but generates an effective momentum-dependent magnetic field (depending on the real magnetic field). Secondly, despite the presence of an effective magnetic field, the Berry curvature is zero here since the out-of-plane Zeeman interaction is overwhelmed by disorder. Thirdly, quantum mechanical effects in charge transport, such as weak localization [61] and the Altshuler-Aronov terms in the conductivity [62,63], are typically observed in diffusive samples only at very low temperatures. This is true even when the Fermi surface remains isotropic, which occurs if only one of the two Zeeman terms is present. We stress there is no Rashba spin-orbit coupling, while the Dresselhaus interaction will not alter the dependence of the results on the magnitude and orientation of $B_\parallel$.

Figure 3 shows the extrema of ΔR_H as a function of B_x. The correction ΔR_H of the Hall coefficient is maximal when $\phi = \pi/2, 3\pi/2$ and minimal when $\phi = 0, \pi, 2\pi$. For GaAs, the quadratic-k and quartic-k Zeeman interactions are of the same order of magnitude. Hence, ΔR_H changes sign depending on ϕ. In contrast, for InAs, the Zeeman interactions are dominated by the quartic-k Zeeman term, hence its angular dependence of ΔR_H becomes less important than GaAs.

Experimentally, the quadratic-k and quartic-k Zeeman interactions can be distinguished in one-dimensional holes by measuring the directional dependence of the electrical conductance [57] and can be separately determined by magnetic focusing [64]. On the other hand, the correction ΔR_H can be measured via the dependence of R_H on ϕ in 2D holes, without requiring ultralow temperatures, a large magnetic field, or optical setups. Our findings have consequences for quantum computation since electron dipole spin resonance needs both the spin-orbit interaction and a magnetic field for a spin-orbit qubit to be encoded as well as manipulated, and spin blockade depends sensitively on the in-plane magnetic field [34]. A strong Δ_2 would mean that an in-plane magnetic field could be used to tune the Berry curvature and topological properties of two-dimensional holes proximity coupled to a ferromagnet or an antiferromagnet [65]. Furthermore, $B_\parallel$ could also be used to make one band nearly flat, increasing the effect of hole-hole interactions relevant for strongly correlated phases.

We briefly summarize the derivation steps of the magnetotransport coefficients, whose details can be found in the Supplemental Material [66]. The density operator $\hat{\rho}$ obeys the quantum Liouville equation

$$\frac{d\hat{\rho}}{dt} + \frac{i}{\hbar}[\hat{H}, \hat{\rho}] = 0. \tag{3}$$

Projecting the density operator onto the states $\{|\boldsymbol{k}s\rangle\}$, where $\boldsymbol{k}$ is the wave vector and s denotes the spin index, the matrix elements $\hat{\rho}_{\boldsymbol{k}\boldsymbol{k}'} \equiv \hat{\rho}^{ss'}_{\boldsymbol{k}\boldsymbol{k}'} = \langle \boldsymbol{k}s|\hat{\rho}|\boldsymbol{k}'s'\rangle$. Here we assume short-ranged uncorrelated impurities such that the average of potential over impurity configurations is $n_i|U_{\mathbf{k}'\mathbf{k}}|^2/V$, where V is the crystal volume, n_i is the impurity concentration, and $U_{\mathbf{k}'\mathbf{k}}$ is the matrix element of an impurity's potential. The central quantity in transport is the density matrix averaged over impurity configurations, which is also diagonal in wave vector, since the impurity average restores translational periodicity. We denote the impurity-averaged density matrix by $f_{\boldsymbol{k}}$. In the Born approximation for the impurity potential it satisfies the following quantum kinetic equation:

$$\frac{df_{\boldsymbol{k}}}{dt} + \frac{i}{\hbar}[H_{0\boldsymbol{k}} + H_Z, f_{\boldsymbol{k}}] + \hat{J}(f_{\boldsymbol{k}}) = \mathcal{D}_{E,\boldsymbol{k}} + \mathcal{D}_{L,\boldsymbol{k}}, \tag{4}$$

where $H_Z = g\mu_B \boldsymbol{\sigma}\cdot\mathbf{B}$ having g, a material-specific parameter and μ_B, the Bohr magneton, $\hat{J}(f_{\boldsymbol{k}})$ is the scattering term in the Born approximation, given as

$$\hat{J}(f_{\boldsymbol{k}}) = \left\langle \frac{1}{\hbar^2}\int_0^\infty dt' [\hat{U}, e^{-iH_0t'/\hbar}[\hat{U}, \hat{f}(t)]e^{iH_0t'/\hbar}] \right\rangle_{\boldsymbol{k}\boldsymbol{k}}, \tag{5}$$

while $\mathcal{D}_{E,\boldsymbol{k}} = -(1/\hbar)e\mathbf{E}\cdot\partial f_{\mathbf{k}}/\partial\mathbf{k}$ is the driving term due to an applied electric field E and $\mathcal{D}_{L,\boldsymbol{k}} = (e/2\hbar)\{\hat{\mathbf{v}}\times\mathbf{B}, \partial f_{\mathbf{k}}/\partial\mathbf{k}\}$ contains the effect of the Lorentz force due to the out-of-plane magnetic field.

The steady-state solution to Eq. (4) can be found as follows. We perform a perturbation expansion up to first order in the electric and out-of-plane magnetic fields, and up to second order in the in-plane magnetic field, meaning that we keep terms up to order $B_\parallel^2$. Firstly, we decompose $f_{\boldsymbol{k}}$ as $f_{\boldsymbol{k}} = f_{0\boldsymbol{k}} + f_{E\boldsymbol{k}} + f_{L\boldsymbol{k}}$, where $f_{0\boldsymbol{k}}$ is the equilibrium density matrix, $f_{E\boldsymbol{k}}$ is a correction to first order in the electric field when $B_z = 0$, and $f_{L\boldsymbol{k}}$ is an additional correction first order in the electric and out-of-plane magnetic fields. Secondly, we use the equilibrium density matrix $f_{0\boldsymbol{k}}$ in Eq. (4) with zero out-of-plane magnetic field, but finite in-plane magnetic field, to obtain $\mathcal{D}_{E,\boldsymbol{k}}$, from which we obtain $f_{E\boldsymbol{k}}$. Thirdly, using $f_{E\boldsymbol{k}}$ and with only $f_{L\boldsymbol{k}}$ on the right-hand side of Eq. (4), we solve for $f_{L\boldsymbol{k}}$. Finally, the current density is found as the expectation value $\boldsymbol{j}_{x,y} = e\,\mathrm{Tr}[\hat{\boldsymbol{v}}_{x,y}f_{\boldsymbol{k}}]$, with $\hat{\boldsymbol{v}} = (1/\hbar)\,\partial H_{0\boldsymbol{k}}/\partial\boldsymbol{k}$, which yields the conductivity tensor σ.

Following the above procedure, the longitudinal conductivity σ_{xx} can be expressed as

$$\sigma_{xx} = \frac{e^2\tau_p}{2\pi m^*}k_F^2\left\{1 - \left(\frac{m^{*2}B_\parallel^2}{\hbar^4}\right)\left[20\Delta_1^2 + 104k_F^4\Delta_2^2 + 44k_F^2\Delta_1\Delta_2 c_{2\phi} + 2g(\phi)\right]\right\}, \tag{6}$$

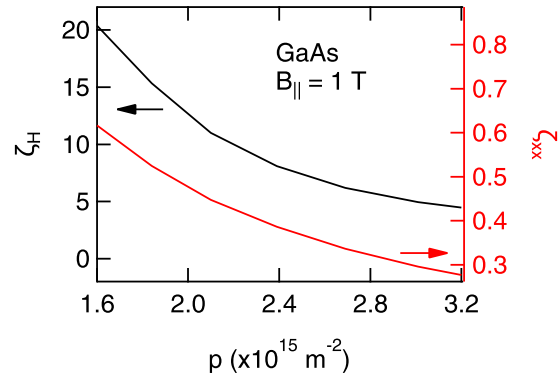

FIG. 4. The anisotropy ζ_H and ζ_{xx} of the Hall resistance and longitudinal conductivity as a function of hole density, defined as $\zeta_H \equiv \frac{\Delta R_H(\pi/2)-R_H(0)}{R_H(0)}$ and $\zeta_{xx} \equiv \frac{\Delta\sigma_{xx}(\pi/2)-\sigma_{xx}(0)}{\sigma_{xx}(0)}$, respectively.

where k_F is the Fermi wave vector and for the case $B_\parallel = 0$, $k_F = \sqrt{2\pi p}$, having p the 2DHG density, and

$$g(\phi) = -\frac{2}{\pi}\int_0^{2\pi} d\theta\, c_\theta \frac{I+J}{G(k_F)}\left(2 - \frac{k_F^2B_\parallel^2\Delta_1}{\sqrt{G(k_F)}}\right) \times \left(2\Delta_1^2 c_\theta + \Delta_1\Delta_2 k_F^2(2c_{3\theta-2\phi} + 4c_{\theta-2\phi}) + 4\Delta_2^2k_F^4c_\theta\right), \tag{7}$$

with $I \equiv \Delta_2^2k_F^8B_\parallel^2$ and $J \equiv \Delta_1\Delta_2k_F^6B_\parallel^2c_{2(\theta-\phi)}$. The complete expressions for the transverse conductivity σ_{xy} and Hall coefficient R_H are given in the Supplemental Material. The expressions for $\Delta\sigma_{xx}$, $\Delta\sigma_{xy}$, and ΔR_H all contain terms $\propto \cos[(\Delta w)\phi]$, where $\Delta w \equiv |w_1 - w_2| = 2$ is the difference in the winding number of the two Zeeman terms. Correspondingly, the period of the anisotropy in the magnetoresistance is $2\pi/(\Delta w) = \pi$, which explains the angular dependence of the magnetoresistance in Figs. 2 and 3.

As expected from the behavior of the dispersion at low and high densities (Fig. 1), the anisotropy in the magnetoresistance is strongly highly density dependent. At very high densities the anisotropy decreases, as seen in Fig. 4, because the quartic Zeeman term $\propto\Delta_2$ overwhelms the quadratic, and the dispersion once again becomes approximately isotropic. Previous experiments probed the density dependence of the total Zeeman splitting in an out-of-plane magnetic field [44]. This work shows that the existence of the quartic term, with a winding number of 4, can be detected by measuring the angular dependence of the in-plane magnetoresistance.

To summarize, we have evaluated the longitudinal conductivity σ_{xx} and low-field Hall coefficient R_H of two-dimensional holes in GaAs and InAs symmetric quantum wells in an in-plane magnetic field, but with no Rashba spin-orbit interaction. In two-dimensional holes the strong spin-orbit interaction gives rise to a Zeeman interaction of the form $(\Delta_1B_+k_+^2\sigma_- + \Delta_2B_-k_+^4\sigma_- + \mathrm{H.c.})$, which causes the velocity operator, and hence σ_{xx}, σ_{xy}, and R_H, to depend strongly on the relative orientation of the electric and magnetic fields. This anisotropy in the magnetoresistance should be easily detected experimentally and should be observable in any materials with spin-orbit terms that have different winding numbers.

Given the generality of our results, we expect that our work will stimulate further studies on the signatures of spin states

in the classical transport properties of strongly spin-orbit coupled systems. Our work also has important implications for electron dipole spin resonance in the context of quantum computing, where the in-plane magnetic field acts as a tunable spin-orbit interaction through which the spin states can be manipulated. Finally, our work shows that one can probe the band topology from the magnetoresistance, with anisotropy period $2\pi/(\Delta w)$ where Δw is the difference in the winding number of the spin-orbit terms. Furthermore, one can determine from the magnetoresistance whether a type of spin-orbit interaction with a given winding number is dominant, or whether there are two spin-orbit terms of comparable magnitude that have a different winding number. In the latter case, the system is close to a point where a topological phase transition can occur.

This work was funded by the Australian Research Council Centre of Excellence in Future Low-Energy Electronics Technologies. We thank Hong Liu and Samuel Bladwell for helpful discussions.

[1] X. L. Qi and S. C. Zhang, Phys. Today **63**(1), 33 (2010).
[2] M. Z. Hasan and C. L. Kane, Rev. Mod. Phys. **82**, 3045 (2010).
[3] A. Kormanyos, G. G. Burkard, M. Gmitra, J. Fabian, V. Zolyomi, and N. D. D. V. Fal'ko, 2D Mater. **2**, 022001 (2015).
[4] N. P. Armitage, E. J. Mele, and A. Vishwanath, Rev. Mod. Phys. **90**, 015001 (2018).
[5] M. J. Manfra, L. N. Pfeiffer, K. W. West, R. de Picciotto, and K. W. Baldwin, Appl. Phys. Lett. **86**, 162106 (2005).
[6] B. Habib, M. Shayegan, and R. Winkler, Semicond. Sci. Technol. **23**, 064002 (2009).
[7] X.-J. Hao, T. Tu, G. Cao, C. Zhou, H.-O. Li, G.-C. Guo, W. Y. Fung, Z. Ji, G.-P. Guo, and W. Lu, Nano Lett. **10**, 2956 (2010).
[8] S. Chesi, G. F. Giuliani, L. P. Rokhinson, L. N. Pfeiffer, and K. W. West, Phys. Rev. Lett. **106**, 236601 (2011).
[9] D. Q. Wang, O. Klochan, J.-T. Hung, D. Culcer, I. Farrer, D. A. Ritchie, and A. R. Hamilton, Nano Lett. **16**, 7685 (2016).
[10] A. Srinivasan, D. S. Miserev, K. L. Hudson, O. Klochan, K. Muraki, Y. Hirayama, D. Reuter, A. D. Wieck, O. P. Sushkov, and A. R. Hamilton, Phys. Rev. Lett. **118**, 146801 (2017).
[11] T. Korn, M. Kugler, M. Griesbeck, R. Schulz, A. Wagner, M. Hirmer, C. Gerl, D. Schuh, W. Wegscheider, and C. Schüller, New J. Phys. **12**, 043003 (2010).
[12] A. Srinivasan, K. L. Hudson, D. Miserev, L. A. Yeoh, O. Klochan, K. Muraki, Y. Hirayama, O. P. Sushkov, and A. R. Hamilton, Phys. Rev. B **94**, 041406(R) (2016).
[13] S. J. Papadakis, E. P. De Poortere, M. Shayegan, and R. Winkler, Phys. Rev. Lett. **84**, 5592 (2000).
[14] R. Winkler, H. Noh, E. Tutuc, and M. Shayegan, Phys. Rev. B **65**, 155303 (2002).
[15] J. van der Heijden, J. Salfi, J. A. Mol, J. Verduijn, G. C. Tettamanzi, A. R. Hamilton, N. Collaert, and S. Rogge, Nano Lett. **14**, 1492 (2014).
[16] F. Nichele, A. N. Pal, R. Winkler, C. Gerl, W. Wegscheider, T. Ihn, and K. Ensslin, Phys. Rev. B **89**, 081306(R) (2014).
[17] T. Ota, K. Ono, M. Stopa, T. Hatano, S. Tarucha, H. Z. Song, Y. Nakata, T. Miyazawa, T. Ohshima, and N. Yokoyama, Phys. Rev. Lett. **93**, 066801 (2004).
[18] K. Ono, D. G. Austing, Y. Tokura, and S. Tarucha, Science **297**, 1313 (2002).
[19] H. Watzinger, C. Kloeffel, L. Vukušić, M. D. Rossell, V. Sessi, J. Kukučka, R. Kirchschlager, E. Lausecker, A. Truhlar, M. Glaser, A. Rastelli, A. Fuhrer, D. Loss, and G. Katsaros, Nano Lett. **16**, 6879 (2016).
[20] J. D. Watson, S. Mondal, G. A. Csáthy, M. J. Manfra, E. H. Hwang, S. Das Sarma, L. N. Pfeiffer, and K. W. West, Phys. Rev. B **83**, 241305(R) (2011).
[21] R. Hanson, L. P. Kouwenhoven, J. R. Petta, S. Tarucha, and L. M. K. Vandersypen, Rev. Mod. Phys. **79**, 1217 (2007).
[22] A. F. Croxall, B. Zheng, F. Sfigakis, K. Das Gupta, I. Farrer, C. A. Nicoll, H. E. Beere, and D. A. Ritchie, Appl. Phys. Lett. **102**, 082105 (2013).
[23] C. Gerl, S. Schmultz, H.-P. Tranitz, C. Mitzkus, and W. Wegscheider, Appl. Phys. Lett. **86**, 252105 (2005).
[24] W. R. Clarke, C. E. Yasin, A. R. Hamilton, A. P. Micolich, M. Y. Simmons, K. Muraki, Y. Hirayama, M. Pepper, and D. A. Ritchie, Nat. Phys. **4**, 55 (2007).
[25] R. Cuan and L. Diago-Cisneros, Europhys. Lett. **110**, 67001 (2015).
[26] T. Biswas, S. Chowdhury, and T. K. Ghosh, Eur. Phys. J. B **88**, 220 (2015).
[27] F. A. Zwanenburg, A. S. Dzurak, A. Morello, M. Y. Simmons, L. C. L. Hollenberg, G. Klimeck, S. Rogge, S. N. Coppersmith, and M. A. Eriksson, Rev. Mod. Phys. **85**, 961 (2013).
[28] S. Conesa-Boj, A. Li, S. Koelling, M. Brauns, J. Ridderbos, T. T. Nguyen, M. A. Verheijen, P. M. Koenraad, F. A. Zwanenburg, and E. P. A. M. Bakkers, Nano Lett. **17**, 2259 (2017).
[29] M. Brauns, J. Ridderbos, A. Li, W. G. van der Wiel, E. P. A. M. Bakkers, and F. A. Zwanenburg, Appl. Phys. Lett. **109**, 143113 (2016).
[30] M. Brauns, J. Ridderbos, A. Li, E. P. A. M. Bakkers, W. G. van der Wiel, and F. A. Zwanenburg, Phys. Rev. B **94**, 041411(R) (2016).
[31] F. Mueller, G. Konstantaras, P. C. Spruijtenburg, W. G. van der Wiel, and F. A. Zwanenburg, Nano Lett. **15**, 5336 (2015).
[32] F. Qu, J. van Veen, F. K. de Vries, A. J. A. Beukman, M. Wimmer, W. Yi, A. A. Kiselev, B.-M. Nguyen, M. Sokolich, M. J. Manfra, F. Nichele, C. M. Marcus, and L. P. Kouwenhoven, Nano Lett. **16**, 7509 (2016).
[33] R. Maurand, X. Jehl, D. K. Patil, A. Corna, H. Bohuslavskyi, R. Laviéville, L. Hutin, S. Barraud, M. Vinet, M. Sanquer, and S. De Franceschi, Nat. Commun. **7**, 13575 (2016).
[34] J.-T. Hung, E. Marcellina, B. Wang, A. R. Hamilton, and D. Culcer, Phys. Rev. B **95**, 195316 (2017).
[35] H. Watzinger, J. Kukučka, L. Vukušić, F. Gao, T. Wang, F. Schäffler, J.-J. Zhang, and G. Katsaros, Nat. Commun. **9**, 3902 (2018).

[36] S. Liles, R. Li, C. H. Yang, F. E. Hudson, M. Veldhorst, A. S. Dzurak, and A. R. Hamilton, Nat. Commun. **9**, 3255 (2018).
[37] R. Winkler, *Spin-Orbit Coupling Effects in Two-Dimensional Electron and Hole Systems* (Springer, Berlin, 2003).
[38] R. Moriya, K. Sawano, Y. Hoshi, S. Masubuchi, Y. Shiraki, A. Wild, C. Neumann, G. Abstreiter, D. Bougeard, T. Koga, and T. Machida, Phys. Rev. Lett. **113**, 086601 (2014).
[39] T. Biswas and T. K. Ghosh, J. Appl. Phys. **115**, 213701 (2014).
[40] K. V. Shanavas, Phys. Rev. B **93**, 045108 (2016).
[41] G. Akhgar, O. Klochan, L. H. Willems van Beveren, M. T. Edmonds, F. Maier, B. J. Spencer, J. C. McCallum, L. Ley, A. R. Hamilton, and C. I. Pakes, Nano Lett. **16**, 3768 (2016).
[42] C. M. Wang, S. Y. Liu, Q. Lin, X. L. Lei, and M. Q. Pang, J. Phys.: Condens. Matter **22**, 095803 (2010).
[43] H. Liu, E. Marcellina, A. R. Hamilton, and D. Culcer, Phys. Rev. Lett. **121**, 087701 (2018).
[44] E. Marcellina, A. Srinivasan, D. S. Miserev, A. F. Croxall, D. A. Ritchie, I. Farrer, O. P. Sushkov, D. Culcer, and A. R. Hamilton, Phys. Rev. Lett. **121**, 077701 (2018).
[45] D. V. Bulaev and D. Loss, Phys. Rev. Lett. **95**, 076805 (2005).
[46] F. Nichele, M. Kjaergaard, H. J. Suominen, R. Skolasinski, M. Wimmer, B.-M. Nguyen, A. A. Kiselev, W. Yi, M. Sokolich, M. J. Manfra, F. Qu, A. J. A. Beukman, L. P. Kouwenhoven, and C. M. Marcus, Phys. Rev. Lett. **118**, 016801 (2017).
[47] J. R. Petta, A. C. Johnson, J. M. Taylor, E. A. Laird, A. Yacoby, M. D. Lukin, C. M. Marcus, M. P. Hanson, and A. C. Gossard, Science **309**, 2180 (2005).
[48] J. Salfi, J. A. Mol, D. Culcer, and S. Rogge, Phys. Rev. Lett. **116**, 246801 (2016).
[49] J. Salfi, M. Tong, S. Rogge, and D. Culcer, Nanotechnology **27**, 244001 (2016).
[50] N. W. Hendrickx, D. P. Franke, A. Sammak, M. Kouwenhoven, D. Sabbagh, L. Yeoh, R. Li, M. L. V. Tagliaferri, M. Virgilio, G. Capellini, G. Scappucci, and M. Veldhorst, Nat. Commun. **9**, 2835 (2018).
[51] R. M. Lutchyn, J. D. Sau, and S. Das Sarma, Phys. Rev. Lett. **105**, 077001 (2010).
[52] J. Alicea, Y. Oreg, G. Refael, F. von Oppen, and M. P. A. Fisher, Nat. Phys. **7**, 412 (2011).
[53] S. T. Gill, J. Damasco, D. Car, E. P. A. M. Bakkers, and N. Mason, Appl. Phys. Lett. **109**, 233502 (2016).
[54] S. V. Alestin Mawrie and T. K. Ghosh, J. Phys.: Condens. Matter **29**, 465303 (2017).
[55] R. Raimondi, M. Leadbeater, P. Schwab, E. Caroti, and C. Castellani, Phys. Rev. B **64**, 235110 (2001).
[56] J. Liang and Y. Lyanda-Geller, Phys. Rev. B **95**, 201404(R) (2017).
[57] D. S. Miserev, A. Srinivasan, O.A. Tkachenko, V. A. Tkachenko, I. Farrer, D. A. Ritchie, A. R. Hamilton, and O. P. Sushkov, Phys. Rev. Lett. **119**, 116803 (2017).
[58] Y. A. Bychkov and E. I. Rashba, J. Phys. C: Solid State Phys. **17**, 6039 (1984).
[59] D. S. Miserev and O. P. Sushkov, Phys. Rev. B **95**, 085431 (2017).
[60] G. Dresselhaus, Phys. Rev. **100**, 580 (1955).
[61] S. Datta, *Electronic Transport in Mesoscopic Systems* (Cambridge University Press, Cambridge, 1995).
[62] B. L. Al'tshuler and A. G. Aronov, Zh. Eksp. Teor. Fiz. **77**, 2028 (1979) [Sov. Phys. JETP **50**, 968 (1979)].
[63] B. L. Altshuler, A. G. Aronov, and P. A. Lee, Phys. Rev. Lett. **44**, 1288 (1980).
[64] S. Bladwell and O. P. Sushkov, Phys. Rev. B **99**, 081401(R) (2019).
[65] T. Dietl and H. Ohno, Rev. Mod. Phys. **86**, 187 (2014).
[66] See Supplemental Material at http://link.aps.org/supplemental/10.1103/PhysRevB.101.121302 for additional details and calculations, which includes Ref. [67].
[67] D. Culcer, A. Sekine, and A. H. MacDonald, Phys. Rev. B **96**, 035106 (2017).